Motion parallax in electric sensing

Federico Pedraja[a,1], Volker Hofmann[a,1,2], Kathleen M. Lucas[b], Colleen Young[b], Jacob Engelmann[a], and John E. Lewis[b,c,3]

[a]Faculty of Biology/Cluster of Excellence Cognitive Interaction Technology, Active Sensing Group, Bielefeld University, D-33501 Bielefeld, Germany; [b]Department of Biology, University of Ottawa, Ottawa, ON, K1N 6N5 Canada; and [c]University of Ottawa Brain and Mind Research Institute, University of Ottawa, Ottawa, ON, K1H 8M5 Canada

Edited by Terrence J. Sejnowski, Salk Institute for Biological Studies, La Jolla, CA, and approved December 8, 2017 (received for review July 11, 2017)

A crucial step in forming spatial representations of the environment involves the estimation of relative distance. Active sampling through specific movements is considered essential for optimizing the sensory flow that enables the extraction of distance cues. However, in electric sensing, direct evidence for the generation and exploitation of sensory flow is lacking. Weakly electric fish rely on a self-generated electric field to navigate and capture prey in the dark. This electric sense provides a blurred representation of the environment, making the exquisite sensory abilities of electric fish enigmatic. Stereotyped back-and-forth swimming patterns reminiscent of visual peering movements are suggestive of the active generation of sensory flow, but how motion contributes to the disambiguation of the electrosensory world remains unclear. Here, we show that a dipole-like electric field geometry coupled to motion provides the physical basis for a nonvisual parallax. We then show in a behavioral assay that this cue is used for electrosensory distance perception across phylogenetically distant taxa of weakly electric fish. Notably, these species electrically sample the environment in temporally distinct ways (using discrete pulses or quasisinusoidal waves), suggesting a ubiquitous role for parallax in electric sensing. Our results demonstrate that electrosensory information is extracted from sensory flow and used in a behaviorally relevant context. A better understanding of motion-based electric sensing will provide insight into the sensorimotor coordination required for active sensing in general and may lead to improved electric field-based imaging applications in a variety of contexts.

active sensing | sensory flow | distance perception | weakly electric fish

To form spatial representations, animals must estimate the relative distance of objects in their environment. Dynamic cues associated with sensory flow can play a key role in this process. In vision, the motion parallax arising from changing viewpoints causes an object's image to move across a photoreceptor array with a speed that is inversely proportional to the object's distance (1, 2). In this way, directed movement generates optic flow that provides important information for distance perception (1–5). Here, we describe how a specific cue for distance perception arises from sensory flow during electric sensing by weakly electric fish.

The physics of electric sensing are similar across many species in the two independently evolved families of electric fish (African Mormyrids and South American Gymnotiforms) (6, 7). These fish produce an electric organ discharge that is shaped by their body into an asymmetric dipole-like electric field (Fig. 1*A*) (8–10). Environmental perturbations of the electric field modulate the spatial pattern of voltage across the fish's skin; this electric image provides a blurry representation of the environment but is nonetheless the sensory basis for object localization, prey capture, and navigation in the dark (11–13). A number of static cues related to the electric image have been linked to electrosensory distance perception (12, 14, 15), but how fish use motion-based sensory flow is not clear. Indeed, the stereotyped "va-et-vient" swimming resembling visual peering movements (16–18) strongly suggests that dynamic cues are extracted through the generation of sensory flow (19–22). In addition, electrosensory neurons encode a wide range of spatiotemporally varying stimuli that could arise from sensory flow (23–25). Interestingly, in the context of looming objects, these neurons have recently been shown to implement a focusing mechanism that correlates well with classic behavioral data (26–28). However, it has not yet been possible to directly test the hypothesis that motion-generated cues are used for electric sensing.

In the following, we describe how the electric image is shaped by a dipole-like electric field geometry such that relative motion generates a cue similar to visual parallax. Then, by manipulating this electrosensory parallax cue in a behavioral assay, we show that both Mormyrid and Gymnotiform species exploit this cue for electrosensory distance perception.

Results and Discussion

To understand the information content of the electric image, we must consider the change in the electric field caused by an object, the "field perturbation" (Fig. 1 *B* and *C*) (9, 12). The field perturbation shows that the object is polarized, with the gradient of the polarization (Fig. 1 *B* and *C*, white arrows) oriented along the electric field lines (black contours, Fig. 1*A*). Due to the changing curvature of the field lines, the polarization gradient rotates toward the midbody as an object moves away from the fish (Fig. 1 *B* and *C*, compare black and white arrows; Fig. S1 and Movie S1). This has marked effects on the electric image (Fig. 1 *D* and *E* and Fig. S2): as the lateral distance of the object increases, the amplitude of the image decreases (compare light to dark curves), while the peak of the image (open circles on each curve) shifts toward the midbody (caudally in Fig. 1*D*, rostrally in

Significance

Through specific movements, animals can structure the dynamics of sensory inputs to optimize perception. In vision, side-to-side peering can provide distance information from visual parallax. Weakly electric fish exhibit swimming patterns reminiscent of visual peering, but there is no direct evidence that these fish use motion-related cues for electric sensing. Indeed, how a dynamic environment is perceived through an electrosensory lens remains unclear. By combining computational modeling and a behavioral test, we demonstrate that temporal dynamics, along with a dipole electric field geometry, generates a parallax-like cue that weakly electric fish from two independent taxa exploit for distance perception. Studying weakly electric fish will lead to a better understanding of active sensing and the fundamental principles of sensory processing.

Author contributions: F.P., V.H., J.E., and J.E.L. designed research; F.P., V.H., K.M.L., and C.Y. performed research; F.P., V.H., J.E., and J.E.L. contributed new reagents/analytic tools; F.P., V.H., K.M.L., J.E., and J.E.L. analyzed data; and F.P., V.H., J.E., and J.E.L. wrote the paper.

The authors declare no conflict of interest.

This article is a PNAS Direct Submission.

[1]F.P. and V.H. contributed equally to this work.

[2]Present address: Department of Physiology, McGill University, Montreal, QC, H3G 1Y6 Canada.

[3]To whom correspondence should be addressed. Email: john.lewis@uottawa.ca.

This article contains supporting information online at www.pnas.org/lookup/suppl/doi:10.1073/pnas.1712380115/-/DCSupplemental.

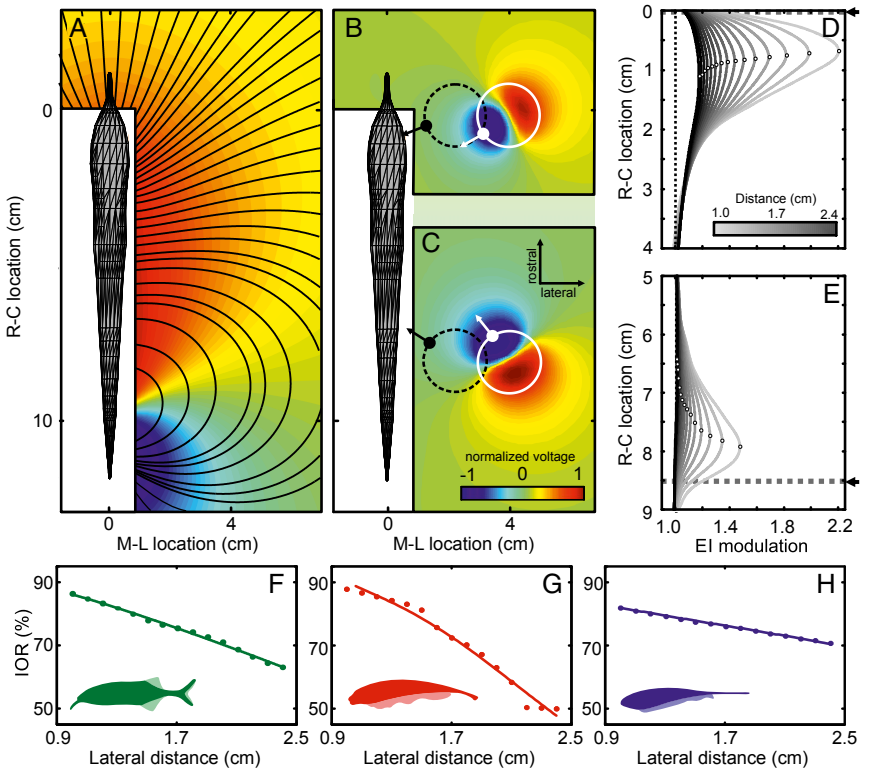

Fig. 1. Physical basis of electrosensory motion parallax. (*A*) *Top* view of the basal electric field of *Gnathonemus petersii* computed using a boundary element method (BEM) electric field model (*Materials and Methods*). Normalized voltage is shown as a color map (red, positive and blue, negative); electric field lines are indicated by black contours. The white areas close to the fish comprise points where data could not be obtained in the corresponding physical measurements (Fig. S2). (*B* and *C*) Electric field perturbations due to a metal sphere (1-cm radius) positioned at two different rostral–caudal locations (*B*, rostral; *C*, caudal) and a lateral distance of 2.9 cm. The field perturbation (plotted as normalized voltage; see color bar) is defined as the difference between the electric field with and without the object present. The position and size of the sphere is indicated by the white circle. The polarization gradient of the object (white arrows) is roughly aligned with the field lines of the unperturbed field (see black contour lines in *A*). Accordingly, the gradient differs by almost 90° for the rostral and the caudal object. The dashed black circles represent the spheres at a distance of 1.1 cm from the fish with the corresponding polarization gradient shown by the black arrows. At this closer lateral distance, the angular difference of the polarization gradients is smaller than when the object is further away (white circles, see also Fig. S1). (*D* and *E*) Electric images (EIs) of the sphere at different lateral distances (1–2.4 cm; see grayscale bar) for the same rostral–caudal positions as in *B* and *C*, respectively. The location of the object along the rostral–caudal axis is indicated by the dashed lines in both panels (fish mouth at x = 0 cm). Note that the amplitude of the EI decreases with increasing lateral distance, while the EI peak (open circles) shifts toward the midbody. (*F–H*) The image–object ratio (IOR) measured using BEM electric field models for three different species. The IOR is the ratio (in percentage) of the shift of the EI peak (Δ_{image}) to the actual physical displacement of the object (Δ_{object}) for the two rostral–caudal object locations shown in *B* and *C*. The IOR decreased with distance in all cases, suggesting that a more distant object would appear to be moving slower during relative motion. Solid lines show power law fits to the measurements: root-mean-square error (RMSE) *Gnathonemus petersii* (green) 0.38%, *Apteronotus albifrons* (red) 1.82%, and *Eigenmannia virescens* (blue) 0.14%.

Fig. 1*E*), even though the true rostral–caudal location of the object is constant (dashed lines and arrow). Therefore, as a fish swims by an object, the electric image travels a length along the skin (Δ_{image}) that decreases systematically with increased lateral distance of the object, even when the actual rostral–caudal translation (Δ_{object}) is constant. We verified this relationship in three species across the lineages of weakly electric fish using the image–object ratio (IOR = $\Delta_{image}/\Delta_{object}$; Fig. 1 *F–H*, Fig. S2, and Movie S2). From the negative slope of the IOR curves, it follows that the electric image of a nearby object will move faster across the body than the image of a more distant object. Thus, the electric field geometry together with relative motion produces a speed-based cue for distance perception that is similar to motion parallax in vision (1, 2).

We next consider whether weakly electric fish actively exploit this electrosensory-based parallax cue. These fish are well known to track the sidewalls of a moving shuttle box while maintaining a centered position (22), reminiscent of natural behaviors such as hovering and active exploration (28). We hypothesized that electrosensory motion parallax is one of the cues used to perform this behavior. To elicit centering behavior, we used a shuttle comprising two Perspex sidewalls, each with a narrow vertical slit that produces an object-like electric image (Fig. 2*A* and Fig. S3; see *Materials and Methods* and *Supporting Information*). If our hypothesis is true, moving one sidewall more slowly than the other should cause the fish to perceive the slower side as farther away and then shift its position toward the slower side to maintain the perception of being centered (Fig. 2*A*). We estimated the magnitude of this shift using the IOR curves for each species (*Supporting Information* and Fig. S4*A*) and predicted that the fish should shift its position by an amount that depends on speed condition (slow side moving at 90% and 70% of the reference side; Fig. 2*C* open circles and Fig. S4 *B–D*).

To test our parallax hypothesis, we video recorded individual fish in the moving shuttle under infrared illumination (*Materials and Methods*). When both sides of the shuttle moved in tandem at the same speed (2 cm·s^{-1}), fish remained centered (Fig. 2*B*, black). When the speed of one of the sides was decreased while remaining in phase with the opposite side, the fish moved closer to the slower side (Fig. 2 *B* and *C*, dark colors: 1.8 cm·s^{-1} or 90% of the reference speed; light colors: 1.4 cm·s^{-1} or 70% speed). This shift in position was reflected in an increased skewness of

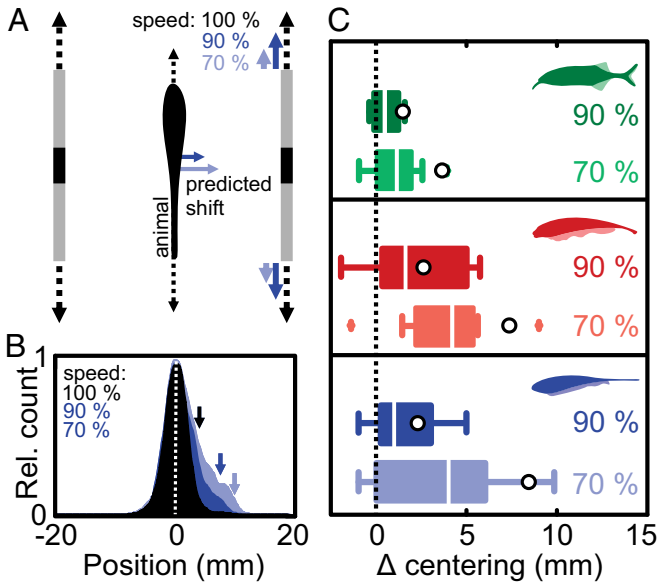

Fig. 2. Behavioral test of the electrosensory parallax hypothesis. (*A*) Schematic drawing of the behavioral setup: *Top* view of a fish positioned between the moving shuttle walls (gray) with a slit (black) acting as a conductive object. Control condition: both sides move back and forth in phase at 2 cm·s^{-1} (dashed black arrows; *Materials and Methods*). Parallax conditions: one side (*Left*) moving at 2 cm·s^{-1} and the other (*Right*) moving in phase at 1.8 cm·s^{-1} (90% speed, blue) or 1.4 cm·s^{-1} (70% speed, light blue). The colored arrows beside the fish indicate the predicted change in centering for each condition under the assumption that electrosensory parallax is used to estimate lateral distance. (*B*) Normalized distributions of fish position during centering behavior in *Eigenmannia*: control condition (n = 21, black), 90% speed (n = 11, dark blue), and 70% speed (n = 10, light blue). Note that for illustrative purposes the position data were adjusted to represent the parallax condition on the *Right*, while the experimental conditions were tested on either side at random. With a stronger parallax cue, the skewness of the position distributions increased as quantified by the 90% quantiles (see arrows). (*C*) Behavioral change in centering for the three species tested (green, *G. petersii*; red, *A. albifrons*; and blue, *E. virescens*). We quantified the behavioral responses as the change in position of the 90% quantile of the position distributions between control and parallax conditions (Δ centering); boxplots show shift in position; median, interquartile range (bars), 1.5 times the interquartile range (whiskers), and outliers (+). For each species, we found a significant shift toward the slower side [Wilcoxon signed-rank test, *G. petersii*: (90%) n = 10, P = 0.04; (70%) n = 9, P = 0.02; *A. albifrons*: (90%) n = 9, P = 0.03; (70%) n = 9, P = 0.01; *E. virescens*: (90%) n = 11 fish, P = 0.02; (70%) n = 10 fish, P = 0.03)]. Open circles represent the predictions of the perceptual shuttle center during parallax conditions based on our EI simulations for each species (*Supporting Information* and Fig. S4).

the position distributions, so we quantified responses using the change in position of the 90% quantile (Fig. 2*B*, see arrows). We found a systematic and significant change in centering in both speed conditions for all species tested (Fig. 2*C*; $F_{3,54}$ = 3.71, P = 0.017). While it is possible that natural centering behavior also involves visual and mechanosensory cues (22, 29, 30), we were able to rule out these influences in our experiments: first, we performed all experiments in the dark, and thus no visual information was available to the fish (31); second, fish did not shift position when provided with mechanosensory cues alone, i.e., when electrosensory cues were absent (Fig. S5). In summary, although the lateral position of the shuttle walls was constant, changing their longitudinal speed caused the fish to move toward the slower side. While these shifts are small (<1 cm), they are behaviorally relevant, as prey detection and the inspection of larger objects occur on similar spatial scales (11, 21).

As predicted, the shift in position differed in magnitude between speed conditions, but there was also variation across individuals and species (Fig. 2*C*). Some of this variability will be due to differences in fish size and details of the electric field geometry, as well as differences in life history (6), neuronal processing (32, 33), or kinematic abilities (20, 30). As in visual depth perception (1, 2), there are also multiple electrosensory cues that could be used in parallel during this centering task (15). Indeed, the skewed distribution of fish positions and smaller-than-predicted shifts suggest that at least one other conflicting cue is involved. One such cue arises from the motion itself. For example, when fish swim faster than the average speed of the two sides of the shuttle, the translation of the electric image (determined by the relative velocity) will in fact be slower on the side of the faster-moving shuttle wall, rather than on that of the slower-moving wall. In this case, the parallax hypothesis predicts a conflicting response: the fish should move toward the faster side of the shuttle (due to its slower relative speed). In general, this occurred only during a fraction of the time (Fig. S6); nonetheless, such a conflict would lead to a behavioral response that is smaller in magnitude than predicted theoretically.

Another cue that fish could use for centering is the electric image amplitude, which is narrower and greater in amplitude when an object is closer (e.g., Fig. 1 *D* and *E*) (12, 34). Thus, an alternative centering strategy could involve comparing the amplitude of the electric image on both sides of the body. If the fish moves toward one side of the shuttle, the image amplitude on that side will increase, so the fish should move in the opposite direction to compensate. Importantly, this strategy is based on a static cue and is independent of the sensory flow (relative motion) required for parallax. Therefore, in our centering assay, in which only the speed of the shuttle-wall changes, this "amplitude hypothesis" predicts that fish should remain centered under all speed conditions. To further explore this possibility, we performed a series of experiments during which such amplitude and parallax-based cues were in competition. Indeed, when the amplitude cue alone was presented, fish moved away from the larger amplitude stimulus (Fig. S7). When both parallax and amplitude cues were presented in conflict (i.e., where amplitude and parallax cues predict shifts in opposite directions), the fish shifted to an intermediate position that was biased toward the slower-moving side predicted by the parallax cue (Fig. S7). These results confirm that fish use multiple cues during centering behavior; however, future work will be required to determine how these sensory cues are integrated. That said, a stochastic switch between parallax-based and amplitude-based centering strategies could underlie the skewed position distributions observed experimentally (*Supporting Information* and Fig. S8). Additional competing or complementary influences may be involved as well. When a fish scans an object, the spatial aspects of the electric image are transformed into a local temporal pattern of input to the skin electroreceptors (the temporal electric image). Closer objects, with narrower images, lead to higher rates of change in this temporal input (19, 21). Importantly, the temporal electric image and motion parallax cues are inseparable, due to their mutual dependence on electric field geometry: motion parallax increases the speed of image translation for closer objects and thus increases the rate of change of the temporal electric image. In conclusion, our behavioral results can be explained by a centering strategy that uses electrosensory parallax and at least one other electrosensory-based cue.

The two lineages of weakly electric fish have independently evolved electrosensory systems, but have similar electric field geometries (6, 8, 9). We describe an electrosensory parallax that arises directly from the electric field geometry and provide behavioral evidence that fish use this cue to estimate distance. The fact that independently evolved species exhibit similar behavioral responses strongly suggests that electrosensory parallax is a

robust cue for electric sensing. Both lineages exhibit similar stereotypical swimming movements (e.g., va-et-vient scanning) during electrosensory-based behaviors (11, 17, 18, 20, 22). Such motion will generate the electrosensory flow that leads to motion parallax (19, 21, 22), but how the electric fish brain controls the necessary movements remains unknown. The neural coding of image shape and motion is very different between pulse-type Mormyrid (*Gnathonemus*) and wave-type Gymnotiform (*Apteronotus* and *Eigenmannia*) fish; the sensory encoding stage primarily involves a latency code in the former and a rate code in the latter (35). Recent studies have identified motion sensitive neurons in the midbrain of a Gymnotiform fish (36). The responses of these neurons are likely optimized by specific swimming movements (19, 22, 37), but how they might be involved in distance perception is not clear. Interestingly, the centering behavior performed by electric fish is similar to that exhibited by flying insects (4) and walking humans (3, 5, 38, 39), where flow from the right and left visual fields is thought to be actively balanced. Our results suggest that electric fish use a similar strategy during centering behavior; shifting to the slower side effectively increases the speed of electric image translation on that side, therefore balancing the perceived electrosensory flow on both sides of the animal. A better understanding of such strategies, as well as the cues available for electric field-based sensing, will provide important insight into the worlds of electrosensory animals and may also lead to better sensing systems for robotics, human–computer interfaces, and medical imaging.

Materials and Methods

Animals. Wild-caught *Gnathonemus petersii* [either sex, 10–15 cm body length (bl)] and *Eigenmannia virescens* (either sex, 8–15 cm bl) as well as captive-bred *Apteronotus albifrons* (either sex, 9–14 cm bl) were obtained from commercial fish dealers and housed in groups of 5–10 in aerated flow-through tanks. Water temperature was 24–29 °C and water conductivity between 150–300 $\mu S \cdot cm^{-1}$ with a light (L)–dark (D) cycle of 12L:12D. Fish were fed blood worms to satiation three times per week. All procedures for animal maintenance and preparations comply with the current animal protection law of the Federal Republic of Germany, approved by the local authorities Landesamt für Natur, Umwelt und Verbraucherschutz Nordrhein-Westfalen: 87–51- 04.2010.A202 and by the University of Ottawa Animal Care Committee (protocols BL-229 and BL-1773).

Measuring the Electric Field and Electric Image. To record and map the electric field [electric organ discharges (EODs); Fig. S2], animals were initially anesthetized with Hypnomidate (2 $mg \cdot L^{-1}$; Janssen-Cilag) as in previous studies (40). Under this anesthesia, fish ventilate autonomously and show a reduced and regularized EOD rhythm while leaving EOD waveform and EOD amplitude unaltered. Following anesthesia, fish were moved to the experimental tank (Perspex tank 30 × 30 × 15 cm; 100 $\mu S \cdot cm^{-1} \pm 5\ \mu S \cdot cm^{-1}$) and restrained in a holding apparatus, with anesthesia maintained at a lower dose (1 $mg \cdot L^{-1}$). At the end of the experiment, fish recovered quickly upon transfer to a recovery tank containing fresh water.

To record the electric field of *Gnathonemus* ($n = 5$) a custom-built tetrode (X–Y–Z and reference; pairwise spacing of electrodes was 5 mm) was moved in a plane alongside the fish's dorsoventral axis by aid of a computer-controlled cantilever with a step motion profile (steps of 2.5 mm). At each position, at least eight EODs were recorded for the rostrocaudal, mediolateral, and dorsoventral planes. EODs were amplified (10× Gain Cyberamp; Axon Instruments), conditioned (band-pass filter 100 Hz–10 kHz, Cyberamp; Axon Instruments) and digitized (250 kHz, PCIe-6341; National Instruments) using MatLab (Spike Hound v1.2, Gus Kbott III; for Matlab 2015a; The MathWorks, Inc). The voltage gradient was determined by calculating the average peak-to-peak amplitude of all EODs recorded at a given position.

To record electric images (EIs) (Fig. S2) in *Gnathonemus* ($n = 5$) a dipole electrode (spacing of 1 mm) oriented perpendicular to the fish's skin was used. The lateral distance of this electrode was fixed and adjusted to the closest possible distance between the electrode and the animal's skin. The electrode was then moved along the rostrocaudal axis at this fixed lateral distance. The electrode's position was stored for every EOD recorded along the trajectory. From this, we obtained the mean EOD peak-to-peak amplitude as a function of rostrocaudal position of the electrode, which was fitted using a smoothing spline (Matlab 2015a). This procedure was carried out without an object (unperturbed) and with an object (metal sphere, 1-cm radius) introduced at a defined rostrocaudal location and at different lateral distances (perturbed). From this, the EI was calculated as the ratio of the perturbed and the unperturbed EI profile. All distances (experimental and modeling results) refer to the distance between the midbody axis of the fish and the surface of the object.

Modeling the Electric Field and Electric Image. Two different approaches were used to model the electric fields and EIs. The results shown in Fig. 1 and Figs. S1 and S2 were calculated using the boundary element method (BEM) (10, 21, 41); the electric images were calculated as described for the experimental data (modulation of perturbed vs. unperturbed condition). To calculate the electric images produced by the Perspex shuttle (*Supporting Information* and Fig. S3), we used a previously described finite-element model (FEM) for the electric field of *Apteronotus* (42, 43). The FEM approach is more suitable for complex heterogeneous geometries, such as those involved in the shuttle. However, since detailed FEM descriptions for *Gnathonemus* and *Eigenmannia* are not currently available, we used the BEM for all species comparisons.

Behavioral Experiments. Weakly electric fish track and center between pairs of moving vertical rods (44), Perspex plates (28), and window gratings of a Perspex shuttle box (22) using their electric sense. We took a hybrid approach, using two parallel (15 cm long and 8 cm high) Perspex plates with either a vertical cutout (slit; 6 mm width) or a vertical aluminum stripe of similar dimensions (6 mm width, 1 mm thick). As described in the *Supporting Information*, we found that a slit (or aluminum stripe) in such a plate mimics a vertical rod from an electrosensory point of view (Fig. S3), but the Perspex plate had the advantage of increasing the reliability of centering.

Fish were moved to a test tank (61.4 × 31.8 × 31 cm for *Eigenmannia* and 49.6 × 29.6 × 20 cm for *Apteronotus* and *Gnathonemus*) with a water level of 10 cm, temperature of 23–29 °C, and water conductivity of 185–230 $\mu S \cdot cm^{-1}$ (*Eigenmannia*) and 100–110 $\mu S \cdot cm^{-1}$ (*Gnathonemus* and *Apteronotus*). The two Perspex plates were positioned in the middle of the test tank, in parallel and 4 cm apart (Fig. 2*A*). In experiments with *Eigenmannia*, the movement was generated with linear actuators and controlled with custom software (PROmech LP28, Parker.com with Labview, NI.com), while for *Apteronotus* and *Gnathonemus*, plates were moved by the aid of EPOS2 24/5 hardware and actuators (Maxon Motor GmbH) controlled with custom software (Matlab 2015a). In the control condition, both plates moved in phase with a speed of 2 $cm \cdot s^{-1}$ and a cycle period of 6 s (*Eigenmannia*) or 8 s (*Apteronotus* and *Gnathonemus*), such that the range of movement was ±3 cm or ±4 cm. In the test conditions, one plate was moved at 90% or 70% of the control speed (i.e., 1.8 $cm \cdot s^{-1}$ or 1.4 $cm \cdot s^{-1}$); both plates remained in phase with the same cycle period, while the slower plate moved over a smaller range. Within a session, 12 trials (9 for *Eigenmannia*) were obtained per fish. Between trials, the plates remained stationary (50 s or 30 s for *Eigenmannia*). Parallax trials were randomly presented (70% or 90% speed condition) and alternated with both plates moving at 100% speed. To exclude side biases, each parallax condition was presented on the left and on the right side of the shuttle in random order. All trials were video recorded from above at 30 fps under infrared lighting using a Canon FS30 camcorder (Canon Canada, Inc.) or an AVT Marlin F-131 (Allied Vision Technologies).

Behavioral Analyses. Custom-written Matlab routines and VideoPoint 2.5 analysis software were used to measure the lateral (right–left) and longitudinal (front–back) coordinates of the fish and moving plates every 33 ms (30 fps, *Apteronotus* and *Gnathonemus*) or 200 ms (5 fps, *Eigenmannia*). Data from repeated control trials for an individual fish were pooled. The variable of interest was the lateral position of the fish, which was defined as zero when centered between the two plates, and greater than zero when closer to the slow side (or right side in the control condition; Fig. 2*A*). Histograms of the lateral position were constructed (0.1-mm bins, interpolated to 0.02 mm for plotting; Fig. 2*B*). We quantified the position change between control and parallax trials (i.e., the skew of the position distributions) as the change in position of 90% quantile of the position distribution; in other words, the fish was to the right of this position 10% of the time; Fig. 2*B*, arrows). Choosing a different quantile (i.e., 50% or 95%) produced qualitatively similar results. Statistical analyses on the shifts in position (data in Fig. 2*C*) were performed using multiple linear regression (species and speed condition as explanatory variables) and the Wilcoxon signed-rank test for individual comparisons. The shift data for *Apteronotus* and *Gnathonemus* passed the Shapiro–Wilk normality test ($P = 0.76$ and $P = 0.44$, respectively), but that for *Eigenmannia* deviated slightly ($P = 0.04$), so data were log transformed for the regression analysis. Head positions were used to calculate the speed of longitudinal motion (back and forth) over all fish for control and 70% parallax conditions. These were expressed as absolute speeds with the sign set to express the direction relative to the moving shuttle, i.e., positive speeds indicate

movement of the fish in the same direction as the shuttle, while negative values indicate movement in the opposite direction (Fig. S6).

ACKNOWLEDGMENTS. We thank D. Babineau, M. Kelly, and A. Longtin for helpful discussions during the early stages of this work. This work was supported by a discovery grant from the Natural Sciences and Engineering Research Council of Canada (to J.E.L.), an early researcher award from the Government of Ontario (to J.E.L.), and a grant by the Ministerium für Kultur und Wissenschaft des Landes Nordrhein-Westfalen as part of the research cooperation "MoRitS–Model-Based Realization of Intelligent Systems in Nano- and Biotechnologies" (321-8.03.04.03-2012/02) and the DFG (EN 826/5-1) (to J.E.).

1. Kral K (2003) Behavioural-analytical studies of the role of head movements in depth perception in insects, birds and mammals. *Behav Processes* 64:1–12.
2. Ono H, Wade NJ (2005) Depth and motion in historical descriptions of motion parallax. *Perception* 34:1263–1273.
3. Lee DN (1980) The optic flow field: The foundation of vision. *Philos Trans R Soc Lond B Biol Sci* 290:169–179.
4. Srinivasan MV (2011) Visual control of navigation in insects and its relevance for robotics. *Curr Opin Neurobiol* 21:535–543.
5. Koenderink JJ (1986) Optic flow. *Vision Res* 26:161–179.
6. Moller P (2005) *Electric Fishes: History and Behavior* (Chapman and Hill, London).
7. Lewis JE (2014) Active electroreception: Signals, sensing, and behavior. *The Physiology of Fishes* (CRC Press, Boca Raton, FL), 4th Ed, pp 375–390.
8. Assad C, Rasnow B, Stoddard PK (1999) Electric organ discharges and electric images during electrolocation. *J Exp Biol* 202:1185–1193.
9. Caputi AA, Budelli R (2006) Peripheral electrosensory imaging by weakly electric fish. *J Comp Physiol A Neuroethol Sens Neural Behav Physiol* 192:587–600.
10. Pedraja F, Aguilera P, Caputi AA, Budelli R (2014) Electric imaging through evolution, a modeling study of commonalities and differences. *PLoS Comput Biol* 10:e1003722.
11. Nelson ME, MacIver MA (2006) Sensory acquisition in active sensing systems. *J Comp Physiol A Neuroethol Sens Neural Behav Physiol* 192:573–586.
12. Rasnow B (1996) The effects of simple objects on the electric field of *Apteronotus*. *J Comp Physiol A Neuroethol Sens Neural Behav Physiol* 178:397–411.
13. von der Emde G, Fetz S (2007) Distance, shape and more: Recognition of object features during active electrolocation in a weakly electric fish. *J Exp Biol* 210:3082–3095.
14. von der Emde G, Schwarz S, Gomez L, Budelli R, Grant K (1998) Electric fish measure distance in the dark. *Nature* 395:890–894.
15. Lewis JE, Maler L (2002) Blurring of the senses: Common cues for distance perception in diverse sensory systems. *Neuroscience* 114:19–22.
16. Snyder JB, Nelson ME, Burdick JW, Maciver MA (2007) Omnidirectional sensory and motor volumes in electric fish. *PLoS Biol* 5:e301.
17. Lannoo MJ, Lannoo SJ (1993) Why do electric fishes swim backwards? An hypothesis based on gymnotiform foraging behavior interpreted through sensory constraints. *Environ Biol Fishes* 36:157–165.
18. Toerring MJ, Belbenoit P (1979) Motor programmes and electroreception in mormyrid fish. *Behav Ecol Sociobiol* 4:369–379.
19. Hofmann V, et al. (2013) Sensory flow shaped by active sensing: Sensorimotor strategies in electric fish. *J Exp Biol* 216:2487–2500.
20. Hofmann V, Geurten BRH, Sanguinetti-Scheck JI, Gómez-Sena L, Engelmann J (2014) Motor patterns during active electrosensory acquisition. *Front Behav Neurosci* 8:186.
21. Hofmann V, Sanguinetti-Scheck JI, Gómez-Sena L, Engelmann J (2017) Sensory flow as a basis for a novel distance cue in freely behaving electric fish. *J Neurosci* 37:302–312.
22. Stamper SA, Roth E, Cowan NJ, Fortune ES (2012) Active sensing via movement shapes spatiotemporal patterns of sensory feedback. *J Exp Biol* 215:1567–1574.
23. Krahe R, Maler L (2014) Neural maps in the electrosensory system of weakly electric fish. *Curr Opin Neurobiol* 24:13–21.
24. Stamper SA, Fortune ES, Chacron MJ (2013) Perception and coding of envelopes in weakly electric fishes. *J Exp Biol* 216:2393–2402.
25. Metzen MG, Krahe R, Chacron MJ (2016) Burst firing in the electrosensory system of gymnotiform weakly electric fish: Mechanisms and functional roles. *Front Comput Neurosci* 10:81.
26. Clarke SE, Naud R, Longtin A, Maler L (2013) Speed-invariant encoding of looming object distance requires power law spike rate adaptation. *Proc Natl Acad Sci USA* 110:13624–13629.
27. Clarke SE, Longtin A, Maler L (2015) The neural dynamics of sensory focus. *Nat Commun* 6:8764.
28. Heiligenberg W (1973) Electrolocation of objects in the electric fish Eigenmannia. *J Comp Physiol* 87:137–164.
29. Nelson ME, MacIver MA, Coombs S (2002) Modeling electrosensory and mechanosensory images during the predatory behavior of weakly electric fish. *Brain Behav Evol* 59:199–210.
30. Sutton EE, Demir A, Stamper SA, Fortune ES, Cowan NJ (2016) Dynamic modulation of visual and electrosensory gains for locomotor control. *J R Soc Interface* 13:20160057.
31. Ciali S, Gordon J, Moller P (1997) Spectral sensitivity of the weakly discharging electric fish *Gnathonemus petersi* using its electric organ discharges as the response measure. *J Fish Biol* 50:1074–1087.
32. Bell C, Maler L (2005) Central neuroanatomy of electrosensory systems in fish. *Electroreception*, eds Bullock TH, Hopkins CD, Popper AN, Fay RR (Springer, New York), pp 68–111.
33. Caputi AA, Carlson BA, Macadar O (2005) Electric organs and their control. *Electroreception*, eds Bullock TH, Hopkins CD, Popper AN, Fay RR (Springer, New York), pp 410–451.
34. Engelmann J, et al. (2008) Electric imaging through active electrolocation: Implication for the analysis of complex scenes. *Biol Cybern* 98:519–539.
35. Sawtell NB, Williams A, Bell CC (2005) From sparks to spikes: Information processing in the electrosensory systems of fish. *Curr Opin Neurobiol* 15:437–443.
36. Chacron MJ, Fortune ES (2010) Subthreshold membrane conductances enhance directional selectivity in vertebrate sensory neurons. *J Neurophysiol* 104:449–462.
37. Xiao Q, Frost BJ (2013) Motion parallax processing in pigeon (*Columba livia*) pretectal neurons. *Eur J Neurosci* 37:1103–1111.
38. Duchon AP, Warren WH (1994) Robot navigation from a Gibsonian viewpoint. *Proceedings of IEEE International Conference on Systems, Man and Cybernetics*, Vol 3 (Institute of Electrical and Electronics Engineers, Piscataway, NJ), pp 2272–2277.
39. Serres JR, Ruffier F (2017) Optic flow-based collision-free strategies: From insects to robots. *Arthropod Struct Dev* 46:703–717.
40. Engelmann J, Bacelo J, van den Burg E, Grant K (2006) Sensory and motor effects of etomidate anesthesia. *J Neurophysiol* 95:1231–1243.
41. Rother D, et al. (2003) Electric images of two low resistance objects in weakly electric fish. *Biosystems* 71:169–177.
42. Babineau D, Longtin A, Lewis JE (2006) Modeling the electric field of weakly electric fish. *J Exp Biol* 209:3636–3651.
43. Babineau D, Lewis JE, Longtin A (2007) Spatial acuity and prey detection in weakly electric fish. *PLoS Comput Biol* 3:e38.
44. Bastian J (1987) Electrolocation in the presence of jamming signals: Behavior. *J Comp Physiol A* 161:811–824.